Published in final edited form as:
Biochim Biophys Acta. 2009 October ; 1788(10): 2301–2308. doi:10.1016/j.bbamem.2009.08.007.

Cellular Uptake of Electron Paramagnetic Resonance Imaging Probes Through Endocytosis of Liposomes

Scott R. Burks[a,b], **Eugene D. Barth**[c], **Howard J. Halpern**[c], **Gerald M. Rosen**[b,d], and **Joseph P.Y. Kao**[a,b,*]

[a] Department of Physiology, University of Maryland School of Medicine, Baltimore, Maryland, USA.

[b] Medical Biotechnology Center, University of Maryland Biotechnology Institute and Center for EPR Imaging In Vivo Physiology, University of Maryland, Baltimore, Maryland, USA.

[c] Department of Radiation and Cellular Oncology, and Center for EPR Imaging In Vivo Physiology, University of Chicago, Chicago, Illinois, USA.

[d] Department of Pharmaceutical Sciences, University of Maryland School of Pharmacy, Baltimore, Maryland, USA.

Abstract

Electron paramagnetic resonance imaging (EPRI) allows detection and localization of paramagnetic spin probes in vivo and in real time. We have shown that nitroxide spin probes entrapped in the intracellular milieu can be imaged by EPRI. Therefore, with the development of a tumor-targetable vehicle that can efficiently deliver nitroxides into cells, it should be possible to use nitroxide spin probes to label and image cells in a tumor. In this study, we assess the potential of liposomes as a delivery vehicle for imaging probes. We demonstrate that liposomes can stably encapsulate nitroxides at very high concentrations (> 100 mM), at which nitroxides exhibit concentration-dependent quenching of their EPR signal—a process analogous to the quenching of fluorescent molecules. The encapsulating liposomes thus appear spectroscopically “dark”. When the liposomes are endocytosed and degraded by cells, the encapsulated nitroxides are liberated and diluted into the much larger intracellular volume. The consequent relief of quenching generates a robust intracellular nitroxide signal that can be imaged. We show that through endocytosis of nitroxide-loaded liposomes, CV1 cells can achieve intracellular nitroxide concentrations of ~1 mM. By using tissue phantom models, we verify that this concentration is more than sufficient for in vivo EPR imaging.

Keywords

nitroxide; EPR; imaging; liposome; CV1; cellular uptake; signal-generation

1. Introduction

The ability to image a population of cells on the basis of their unique physiology is of clinical importance. For example, tumor imaging enables detection of both primary lesions and secondary sites of metastasis. Low–frequency electron paramagnetic resonance imaging (EPRI) may be an ideal choice for an imaging modality, in light of recent developments that allow non-invasive detection and localization of paramagnetic free radical species in vivo [1, 2]. Endogenous free radicals, being short-lived and of very low abundance, cannot be detected

* Correspondence to: Joseph P.Y. Kao Medical Biotechnology Center University of Maryland Biotechnology Institute 725 W. Lombard St., Baltimore, MD 21201 jkao@umaryland.edu.

in vivo by EPRI. In order to visualize a tissue by EPRI, it is necessary to develop stable free radicals (paramagnetic spin probes) that can target and label tumor tissue. The power of EPRI, particularly using nitroxide probes, stems from the ability to provide read-out on multiple functional aspects of tumor tissue, including tissue oxygen tension [1,3], microviscosity—a measure of how easily small molecules can diffuse locally [4], pH [5], thiol concentration [6], and redox status [7].

We have demonstrated that anionic nitroxide radicals can be loaded intracellularly to millimolar levels [8], and that nitroxides at submillimolar concentrations are imaged with high signal-to-noise ratio by EPRI [4,9]. Although simple anionic nitroxides can be readily loaded into cells, efficient extrusion from cells by organic anion transporters reduces their intracellular retention time at 37 °C [10]. Through rational structural designs that evade extrusion by cellular anion transporters [10], we have extended the intracellular retention times of anionic nitroxides to make EPR imaging studies feasible. For example, (2,2,5,5-tetramethylpyrrolidin-1-oxyl-3-ylmethyl)amine-*N*,*N*-diacetic acid (nitroxide **1**; Fig. 1) has an intracellular exponential lifetime ($t_{1/e}$ or τ) of just under 2 hours at 37°C—sufficiently long to permit EPR imaging.

In earlier studies, we loaded carboxyl-bearing nitroxides into cells through incubation with the corresponding acetoxymethyl (AM) ester, which are labile to hydrolysis by intracellular esterases [8]. During incubation, the AM esters, being nonionic and lipophilic, enter cells by diffusing across the cell membrane. Once inside, cellular esterases rapidly cleave the AM esters to unmask the carboxylates which, being anionic, are retained inside cells. Although the AM ester loading method works very well with cells in vitro, the method is unsuitable for targeted delivery of imaging probes in vivo for two reasons. First, small exogenous molecules like AM esters are rapidly cleared from the circulation [11], which minimizes tissue exposure and thus cellular loading. Second, because intracellular esterases are ubiquitous and AM esters can permeate into all cells, the AM ester loading method cannot target a specific tissue or cell type.

Liposome-based technologies have previously been used to enhance selective uptake of chemotherapeutics into tumor cells and minimize uptake by healthy tissue [12-14]. We wish to investigate whether liposomes are also capable of delivering sufficient concentrations of nitroxides to cells for EPR imaging. Liposomes are an attractive vehicle for delivering EPR imaging probes to cells, as both nitroxides and fluorphores can be sequestered at high (mM) concentrations in the aqueous lumen of the liposome [15,16]. Liposomally encapsulated nitroxides have been used previously to assess the stability of liposomes as drug carriers, [17,18] and as a component in a system for in vitro cellular oxygen measurements [19]. Liposomally encapsulated fluorophores have been widely used to investigate phenomena such as the pH along endosomal pathways [16,20,21]. CV1 cells derived from African Green Monkey kidney epithelium preferentially internalize liposomes that bear negatively-charged lipid head groups through clathrin-dependent endocytosis [22,23]; subsequent disruption of the liposomes in the endocytic pathway releases the contents of the liposomes into the intracellular milieu [22]. As a model for studying the feasibility of using liposomes for cellular delivery of EPR imaging probes, CV1 cells are ideal because they preferentially endocytose liposomes bearing negative surface charge 20 times faster than neutral liposomes [24].

For in vivo applications, imaging probes inside unendocytosed liposomes in circulation could contribute undesirable background signal. Encapsulating nitroxides in liposomes presents a mechanism to circumvent this problem. It is possible to minimize this background by exploiting self-quenching—a concentration-dependent loss of spectroscopic signal that occurs in both nitroxides and fluorophores. When encapsulated at high concentrations inside liposomes, the imaging probes self-quench and are thus spectroscopically “dark” and thus invisible by EPRI. After cellular uptake, disruption of the liposomes releases the probes into the cellular volume. The consequent dequenching of the imaging probes would make the cells “bright” and visible

by EPRI. Liposomal endocytosis and dequenching of imaging probes creates a cell-activated signal-generating mechanism.

In the present study, we show that imaging probes such as nitroxide **1** and 6-carboxyfluorescein can be stably encapsulated in liposomes at sufficiently high concentrations to maximize self-quenching. Upon cell-specific endocytosis, release of imaging probes into the intracellular environment relieves self-quenching to generate robust intracellular spectral signals. Furthermore, we show that through liposomal delivery, nitroxide **1** can accumulate intracellularly to concentrations that are sufficient to enable EPR imaging at high signal-to-noise ratio (SNR).

2. Materials and Methods

2.1. General Materials and Methods

2,2,5,5-Tetramethylpyrrolidin-1-oxyl-3-ylmethyl)amine-*N*,*N*-diacetate dipotassium salt (nitroxide **1**) was synthesized as previously described [10]. 6-Carboxyfluorescein (CF) and 3-carboxy-2,2,5,5-tetramethyl-1-pyrrolidinyloxyl (nitroxide **2**) were from Sigma (St. Louis, MO). The potassium salts of CF and nitroxide **2** were generated by adding appropriate equivalents of KOH. For CF, 0.3 mL of 1 M KOH was added to 0.0376 g CF, and the sample was made to a final concentration of 100 mM with deionized water. For nitroxide **2**, 0.15 mL 1 M KOH was added to 0.0279 g of nitroxide, and the mixture was made to a final concentration of 150 mM. Cell culture media and biochemicals were from Invitrogen (Carlsbad, CA). Fetal bovine serum (FBS) was from Atlanta Biologicals (Lawrenceville, GA). All animal protocols were approved by the Institutional Animal Care and Use Committee at the University of Chicago. Data analyses and presentation were performed with Origin 8.0 (OriginLabs, Northampton, MA), Matlab 2007a (The MathWorks, Natick, MA), and Adobe Photoshop CS3 (Adobe Corp., San Jose, CA).

2.2. Statistical Analysis

One-way ANOVA analysis was used to determine differences among data sets containing more than two groups. A 95% confidence interval ($p < 0.05$) was used to determine significance, and post-hoc analysis was performed according to the Scheffe method of means comparison. All values presented are mean values ± standard deviation.

2.3. Liposome Preparation

Liposomes were composed of 1,2-distearoylphosphatidylcholine (DSPC), cholesterol (Chol), L-α-phosphtidylserine (PS; porcine brain isolate), and 1,2-dipalmitoyl-phosphatidylethanolamine-*N*-(lissamine rhodamine B sulfonyl) ammonium salt (Rhod–PE) in the molar ratio 3:2:0.3:0.003 (DSPC:Chol:PS:Rhod–PE). All lipids were obtained from Avanti Polar Lipids (Alabaster, AL). Where noted, liposomes were made without the addition of PS or Rhod–PE. A solution of 10 μmol phospholipid in 100 μL EtOH was injected into 1 mL of rapidly-stirred aqueous solution of 100 mM CF or 150 mM nitroxide **1** (pH 8.0-8.5). The mixture was extruded 11 times through a 100-nm porosity filter membrane in a Mini Extruder (Avanti Polar Lipids) to yield a suspension of liposomes. All solutions and the extruder were maintained at > 55 °C to ensure fluidity of the lipid phase. Liposomes were purified with Sephadex G-50 resin (~4 g, GE Healthcare, Piscataway, NJ), which was hydrated with H_2O, packed into a FlexColumn (15 mm × 300 mm, Kimbal-Kontes, Vineland, NJ), and equilibrated with Dulbecco's Phosphate Buffered Saline (DPBS) containing Ca^{2+} and Mg^{2+}. Gel filtration yielded ~4 mL of purified liposome suspension in DPBS (final phospholipid concentration ~2 μmol/mL), which was stored at 4° C until use. Phopholipid concentration was determined using the phosphate analysis protocol of Bartlett [25].

2.4. Liposomal Encapsulation Measurements

Liposomes encapsulating quenched CF or nitroxide **1** were measured for fluorescence or EPR spectroscopic signal respectively. Identical spectral measurements were made before and after lysis. Lysis was achieved by the addition of 240 μM digitonin, heating to 95° C for 30 sec, and sonication for 1 min. To assess long-term stability of liposomes encapsulating CF or nitroxide **1**, a reference fluorescence or EPR spectrum was acquired immediately after preparation; the liposomes were then incubated at 37 °C in 90% DPBS–10% FBS, or in 5% DPBS–95% FBS (all percentages by volume). Aliquots were taken at various times thereafter for spectroscopy. Any leaked probe would be dequenched and thus increase the spectroscopic signal above the initial reference baseline value. At each time point, the percentage difference between the "leak signal" and total signal (measured after lysis) represents the fraction of probe still encapsulated in liposomes.

2.5. Cell Culture

CV1 cells (ATCC, Manassas, VA) were maintained at 37 °C in Dulbecco's Modified Eagle Medium (DMEM) supplemented with 10% (v/v) FBS, 2 mM L-glutamine, 100 units/mL penicillin, and 100 μg/mL streptomycin, under a 5% CO_2 atmosphere.

2.6. Cellular Uptake of Liposomes Loaded with CF

CV1 cells (~8×10^4) were plated on 25-mm round No. 1 glass coverslips for 24 – 48 hr. Liposomes encapsulating 100 mM CF were prepared with or without PS, and diluted to a concentration of 0.05 μmol of phospholipid in 2 mL Hanks' Balanced Salt Solution (HBSS). Cells were incubated with liposome suspensions at 37 °C for 2 hr, and then washed thrice with Ca^{2+}- and Mg^{2+}-free HBSS containing 1 mM EDTA. Thereafter, the cells were maintained in normal (Ca^{2+}- and Mg^{2+}-containing) HBSS for fluorescence microscopy.

2.7. Cellular Uptake of Liposomes Loaded with Nitroxide

Replicate 60-mm plastic Petri dishes of CV1 cells were incubated at 37 °C with a suspension of liposomes encapsulating 150 mM nitroxide **1**. Liposomes were at a concentration of 0.1 μmol of phospholipid in 4 mL HBSS. At each time point, cells were washed with HBSS and then released from the plate with trypsin-EDTA solution. Cells were centrifuged at 145 × *g* for 3 min, and the pellet was washed twice with Ca^{2+}- and Mg^{2+}-free HBSS containing 1 mM EDTA. After the final wash, the pellet was resuspended in 400 μL normal HBSS. Cells were lysed with 120 μM digitonin and sonicated for 1 min. Nitroxide and Rhod-PE in the lysates were analyzed by EPR and fluorescence spectroscopy, respectively. The nitroxide concentration in each 400-μL sample was determined using a calibration curve of spectral intensity vs. nitroxide concentration. Control dishes of cells were trypsinized, washed, and counted to determine the average number of cells in each dish (6.25×10^5 cells); total intracellular volume was estimated using a previously estimated intracellular volume of 1.3×10^{-12} L/cell [26]. The average intracellular nitroxide concentration was then estimated through volumetric calculations.

2.8. Implantation of Agarose Cylinder Phantom in an Anesthetized Mouse

A 4% (w/v) agarose solution in PBS was heated to boiling in a microwave oven (~60 sec). Nitroxide **2** was rapidly mixed into the hot agarose to a final concentration of 400 μM. The solution was immediately drawn into a plastic serological pipette with a diameter of 6 mm and allowed to cool to room temperature. The agarose gel was removed from the pipette and cut into 10.2-mm-long cylinders. A cylinder was sealed with a thin coat of Vetbond (3M Corporation, St. Paul, MN) and surgically implanted in the leg of a C3H/HeN:Hsd mouse anesthetized with 3.5% isoflurane inhalant in air. Immediately prior to imaging, the mouse was euthanized with 5% isoflurane for 10 min.

2.9. EPR Spectroscopy

A quartz flat-cell cuvette was used for acquisition of EPR spectra in an X-band spectrometer (E-109, Varian Associates, Palo Alto, CA) at the following settings: microwave power, 20 mW; frequency, 9.55 GHz; field center, 333.5 mT; modulation amplitude, 0.05 mT; modulation frequency, 100 kHz; time constant, 0.5 sec. A field range of 8 mT was scanned in 180 sec. EWWIN software (Scientific Software Services, Plymouth MI) was used for data acquisition. Reported spectral intensity represents the peak-to-peak amplitude of the center line in the 3-line nitroxide spectrum.

2.10. Fluorescence Spectroscopy

Fluorescence spectra were recorded on a dual-excitation spectrofluorometer (model CM1T-10I, SPEX Industries, Metuchen, NJ). Instrument control and data acquisition were performed with Datamax software (Galactic Industries Corporation, Salem, NH). Emission and excitation spectra were acquired to determine optimal wavelength settings (6-carboxyfluorescein: λ_{ex} = 490 nm, λ_{em} = 515 nm; Rhod-PE: λ_{ex} = 550 nm, λ_{em} = 588 nm).

2.11 Fluorescence Microscopy

Fluorescence images were acquired on an inverted epifluorescence microscope (Eclipse TE2000, Nikon Corp, Tokyo, Japan) equipped with a 40× oil-immersion objective (Super Fluor, NA 1.4, Nikon). Excitation light was delivered by a xenon source coupled to a monochromator (PolyChrome II, TILL Photonics, Gräfelfing, Germany). Fluorescence was passed through an appropriate bandpass filter before capture by a CCD camera (CoolSnap HQ, Roper Scientific, Tucson, AZ). MetaFluor software (Molecular Devices, Downingtown, PA) was used for instrument control and image acquisition.

2.12. EPR Imaging and Data Reconstruction

A euthanized mouse with an implanted agarose cylinder impregnated with nitroxide **2** was positioned in the approximate center of the resonant cavity of a 250-MHz EPR imaging spectrometer [27] fitted with a loop-gap resonator with a single loop and a single gap. The sample-holding loop was 25 mm in diameter and 15 mm deep with a loaded Q of 92. A 0.41-mT spectral window encompassed the central spectral peak of the nitroxide. Other instrumental parameters were: RF power, 6 dB; modulation amplitude and frequency, 0.198 mT and 5.120 kHz, respectively; lock-in time constant, 30 ms, with a 30 ms per point dwell time; 256 points per projection; field gradient, 98.1 mT/m.

Continuous wave (CW) EPR intensity images were obtained using an essentially tomographic technique. Projections are defined as field-swept CW spectra in the presence of a 97.3 mT/m gradient, and were obtained in ~8 sec, with 256 points uniformly spaced in the magnetic field. A total of 66 projections were sampled at 10 polar direction angles with multiple azimuthal angles sampled at each polar coordinate. The number of azimuthal projections acquired was dependent on the value of each polar coordinate. As radial distances between azimuthal angles become smaller at higher polar angles, maintaining even spacing between projections required fewer azimuthal angles to be sampled. A filtered back-projection algorithm was used for image reconstruction [28]. Projections were filtered using a simple cutoff of the image response frequency to half the Nyquist sampling limit. Images were reconstructed without correction for the effect of the two other spectral lines not included in the spectral window of 0.23 mT. Since the manifold splittings were greater than 1.4 mT, there was no artifact or sacrifice in resolution.

Spatial resolution of an imaging system is commonly defined by the full-width at half-maximum (FWHM) of a point spread function (PSF). For a phantom cylinder of known

dimensions, the FWHM can be estimated from the edge profile of signal intensity [29]. Briefly, in a two-dimensional slice containing the end-view of the cylinder, 20 intensity profiles uniformly spaced around the circumference of the cylinder were sampled. This was repeated for each of five 2-dimensional slices spaced uniformly along the long axis of the cylinder. The average FWHM determined from the 100 edge profile measurements was 2.6 ± 0.2 mm. The SNR for the phantom cylinder was determined by selecting a region of the image displaying signal and evaluating the mean intensity of the pixels from this region. A region with the same number of pixels outside the signal area was selected and the standard deviation (SD) of the pixel intensity was computed. The SNR, taken as the ratio of the mean intensity in the signal region to the SD outside the region, was 39.

3. Results

3.1. Nitroxides and 6-Carboxyfluorescein Exhibit Concentration-dependent Self-quenching

To document concentration-dependent self-quenching, we recorded the EPR spectra of nitroxide **2** and the fluorescence emission spectra of CF at various concentrations. In Fig. 2, the molar spectroscopic signals of CF and nitroxides are plotted against concentration. For CF, self-quenching becomes detectable at ~50 μM and reaches a maximum at concentrations ~1 mM. With nitroxide **2**, self-quenching is measurable at ~1 mM, and reaches a maximum at ~30 mM. Increasing the luminal concentration in the liposome above these levels does not further increase quenching, but does enable delivery of greater amounts of the imaging probes per liposome.

3.2. Liposomes Encapsulating High Concentrations of Probe are Spectroscopically “Dark”

Liposomes encapsulating either 100 mM CF or 150 mM nitroxide **1** were prepared. Immediately after preparation, liposomes were analyzed by the appropriate spectroscopic method before and after lysis. Lysis of CF-containing liposomes resulted in a 34-fold increase in fluorescence intensity, while lysis of nitroxide-containing liposomes yielded a 90-fold increase in EPR signal intensity (n = 3; Fig 3A). For the suspension of nitroxide-containing liposomes, the EPR spectra acquired before and after lysis are shown in Fig 3B (black and red traces, respectively). These spectra confirm that nitroxides at high concentration inside intact liposomes show only a feeble spectroscopic signal, but when released from lysed liposomes and diluted into bulk solution, the nitroxides give a robust spectral signal. This means that intact liposomes containing high concentrations of nitroxide show minimal EPR spectral signal, and are thus spectroscopically “dark”. Furthermore, this implies that the release and dequenching of nitroxides following disruption of endocytosed liposomes could be an effective means for generating intracellular spectral signal to make the cells appear “bright” in EPR imaging.

3.3. Liposomes Encapsulating CF or Nitroxides are Stable

The suitability of liposomes as nitroxide delivery vehicles depends on their stability. To assess long-term stability of liposomes encapsulating CF or nitroxide **1**, a reference fluorescence or EPR spectrum was acquired immediately after preparation; the liposomes were then incubated at 37 °C in one of two solutions: 1) 90% DPBS–10% FBS, or 2) 5% DPBS–95% FBS. Aliquots were taken at various times thereafter for spectroscopy. Any leaked probe would be dequenched and thus increase the spectroscopic signal above the initial reference value. At each time point, the percentage difference between the “leak signal” and total signal (measured after lysis) represents the fraction of probe still retained in liposomes. Fig. 4 shows fractional probe retention as a function of time for both CF- and nitroxide-containing liposomes. In 90% DPBS–10% FBS, CF–containing liposomes are exceptionally stable. The retention time course is well fit by a line with a slope of -2.0×10^{-4} %/hr (n = 3). Thus, there is negligible leakage of CF even after 24 hours. For liposomes encapsulating nitroxide **1**, in 90% DPBS–10% FBS, the

retention time course follows a first-order exponential decay to a limiting retention of 85.2%, with a lifetime of $\tau = 8.7$ hr (n = 3). Even in 5% DPBS–95% FBS, CF–containing liposomes remain quite stable. The retention time course is well fit by a line with a slope of -0.12 ± 0.011%/hr (n = 3), i.e., less than 3% leakage after 24 hours. In 90% DPBS–10% FBS, liposomes encapsulating nitroxide **1** are somewhat less stable: The retention time course follows a first-order exponential decay to a limiting retention of 82.1%, with a lifetime of $\tau = 0.81 \pm 0.068$ hr (n = 3). These results indicate that during the 7 hours in which cells are incubated with liposomes, the retention of encapsulated nitroxide is > 91% in 90% DPBS–10% FBS (and would be > 82% in 5% DPBS–95% FBS). Therefore, as vehicles for nitroxide delivery, liposomes can be considered stable. For all subsequent experiments, cells were incubated with liposomes in aqueous media containing 10% FBS.

3.4. Dequenching of Liposome-encapsulated CF Generates Intense Intracellular Fluorescence

Liposomes incorporating Rhod–PE, encapsulating 100 mM CF, and having either negative or no surface charge (i.e., with or without PS) were incubated with CV1 cells for 2 hr. After incubation, the cells received three brief washes with Ca^{2+}- and Mg^{2+}-free PBS containing 2 mM ethylenediamine tetraacetate (EDTA) to remove unendocytosed liposomes. CF and Rhod-PE associated with the cells were visualized by fluorescence microscopy (Fig 5). When CV1 cells are incubated with negatively-charged (PS-bearing) liposomes at 37 °C (Fig. 5A – 5C), intense, featureless green fluorescence is observed throughout the cells, indicating internalization and dequenching of the liposome-encapsulated CF. Additionally, robust but structured red fluorescence of Rhod-PE is also visible inside the cells. This reflects incorporation of the Rhod-PE lipids in the liposomes into cellular membranes, and therefore confirms cellular uptake of the liposomes. In contrast, when CV1 cells are incubated at 37 °C with neutral liposomes (incorporating no PS), which are not rapidly endocytosed by CV1 cells [30], only very feeble CF and rhodamine fluorescence could be detected inside cells (Fig. 5D – 5F). Finally, when CV1 cells are incubated with negatively-charged liposomes at 4 °C to block endocytosis [31], no intracellular fluorescence is visible (Fig. 5G – 5I). These results indicate that endocytic uptake of liposomes can be robust, and that relief of self-quenching of liposome-encapsulated imaging probes is a means to generate bright intracellular signal.

3.5. Endocytosis of Liposomes Can Achieve High Intracellular Concentration of Nitroxide

Replicate dishes of CV1 cells were incubated at 37 °C with negatively-charged (PS-containing) liposomes incorporating Rhod–PE, and encapsulating 150 mM nitroxide **1**. At various time points, cells were briefly washed thrice with Ca^{2+}- and Mg^{2+}-free PBS containing 2 mM EDTA to remove unendocytosed liposomes, and the amount of nitroxide and Rhod-PE associated with the cells was determined spectroscopically as described in Materials and Methods. Cell-associated nitroxide and Rhod-PE initially increased in parallel with time of incubation (Fig. 6), as expected from endocytic uptake of liposomes and their luminal contents. At 4 hrs after incubation, the average intracellular nitroxide concentration was close to 1 mM. By 7 hr, intracellular nitroxide concentration had declined to ~300 μM, while cell-associated Rhod-PE was unchanged from the level observed at 4 hr. This suggests that beyond 4 hr, endocytosis became very slow. As a result, without continual uptake of liposomes for replenishment, there is a net loss of intracellular nitroxide signal. Intracellular EPR signal can potentially decay by two mechanisms, extrusion from the cell by organic anion transporters [10], and intracellular reduction to the corresponding hydroxylamine [32,33], which has no EPR signal. Even so, intracellular nitroxide concentrations were in the several hundred micromolar range, which should be visible by EPR imaging and permit cellular imaging studies [9].

3.6. Nitroxide-impregnated Implants are Visible by EPRI In Vivo

We prepared agarose cylinders (4% w/w) impregnated with 400 μM nitroxide **2** and measuring 6 mm in diameter and 10.2 mm in length. A cylinder was implanted subcutaneously in the leg of an anesthetized mouse. The mouse was euthanized and immediately placed in the cavity of a 250-MHz EPR spectrometer for imaging. Euthanasia ensured that acquired images were free of motion artifacts. As shown in Fig. 7, the agarose implant is clearly visible in the EPR image. The known geometry of the cylinder is reproduced in the image with a resolution of 2.6 ± 0.2 mm. The nitroxide signal emanating from the cylinder shows high contrast against the surrounding background, and was imaged with SNR = 39. This experiment shows that at 400 μM, nitroxides are easily detectable and very well imaged in biological tissue by EPRI.

4. Discussion

In this study, we demonstrate that nitroxides, as well as fluorophores, can be encapsulated at self-quenching concentrations in liposomes. Such liposomes exhibit only feeble spectral signals, making them appear “dark” in the appropriate imaging modality. Upon endocytosis of the liposomes by cells, the encapsulated imaging probes are released into the much larger intracellular volume and become dequenched. Therefore, cells that have endocytosed liposomes appear “bright” in the appropriate imaging modality.

We showed that cells can avidly endocytose nitroxide-containing liposomes to achieve intracellular nitroxide concentration close to 1 mM (Fig. 6). Thus, liposomes have potential utility for delivering EPR imaging probes to cells efficiently through endocytosis. Importantly, a phantom, consisting of an agarose cylinder impregnated with 400 μM nitroxide and implanted in a mouse, was readily imaged by EPRI at high contrast and with high SNR.

While liposomes are able to deliver high concentrations of EPR imaging probes into cells in vitro, at least two conditions must be met before in vivo EPRI of a physiologically distinct tissue such as a tumor becomes a reality. First, in order to image a tumor with high contrast, the tumor cells must endocytose liposomes much more efficiently than the surrounding healthy tissue. This can be accomplished by making the liposomes “targetable”—that is, they must incorporate biochemical features that cause preferential uptake by the tumor. Second, targetable liposomes must evade physiological clearance mechanisms and persist in the circulation to maximize their targeting potential.

There are several liposomal targeting approaches that require decorating the liposomal surface with markers that induce preferential uptake by tumors. These have been developed mainly for selective delivery of anti-cancer drugs, but could easily be adapted for delivery of EPR imaging agents. One approach is the conjugation of peptides such as penetrin (PEN) or the HIV transactivator of transcription (TAT) peptide to the liposome. This approach is not intrinsically selective for tumor cells, but rather relies on the higher permeability of tumor vasculature to increase extravasation of liposomes into the interstitial space of tumors [34], where TAT or PEN facilitate liposome translocation into tumor cells. Another mechanism that targets tumors selectively is the immunoliposome—a liposome whose surface is decorated with antibody domains directed against internalizable markers on the tumor cell. Immunoliposomes attach to tumor cells by binding cell-surface antigens, which triggers endocytosis. Immunoliposomes have successfully targeted neuroblastomas and melanomas over-expressing disialoganglioside GD_2 [35,36], breast tumors overexpressing the human epidermal growth factor receptor 2 (HER2) [12,37]. Lastly, liposomes bearing ligands such as folate or transferrin have been successfully used to target glioblastomas and the human gastric cancer cell line MKN-45P that over-express the appropriate receptors [38-41].

Liposomes must evade physiological clearance mechanisms and remain in circulation to maximize uptake by the tumor. Liposomes are filtered from the circulation by the reticulo–endothelial system (RES) of the liver and spleen [42]. Clearance by the RES can be retarded by incorporating into the liposome a small proportion of lipid conjugated to a hydrophilic polymer such as poly(ethyleneglycol) (PEG) to form sterically-stabilized liposomes [43]. The extent to which circulation times are lengthened depends on the mole fraction of PEG-conjugated lipids in the liposome. Thus, the circulation times of liposomes can be fine-tuned to suit a specific application. Our preliminary studies have shown that for liposomes encapsulating nitroxide **1**, incorporating 5 mole-percent PEG-conjugated lipids lengthens the exponential retention time from $\tau \approx 6$ hr to $\tau \approx 19$ hr (unpublished observations).

Finally, the EPR images presented here have excellent SNR and a spatial resolution of 2.6 mm. Improvements in both of these parameters can be brought about by rational design of nitroxide imaging agents. For the nitroxides used in this study, hyperfine interactions with the ^{14}N nucleus (spin 1) split the electron resonance into three spectral peaks that are each approximately one third the total intensity. Because EPRI utilizes the amplitude of a single spectral peak, the signal in the rest of the 3-line spectrum is wasted. Isotopic replacement with ^{15}N (spin ½) results in the electron resonance being split into two peaks, which brings a 50% increase in SNR. Hyperfine interactions with protons broaden the EPR lines, with consequent degradation in SNR and resolution. Hyperfine effects of the deuteron are weaker owing to its smaller magnetic moment; therefore, deuteration of the nitroxide would sharpen EPR spectral peaks and thus improve SNR and spatial resolution. These chemical design improvements are being undertaken.

In summary, the present study suggests that it would be feasible to use liposomes for targeted delivery of imaging agents to tumor cells for in vivo EPR imaging.

Acknowledgments

We thank Dr. Boris Epel (University of Chicago) for technical assistance and instruction in analyzing spatial resolution. This work was supported by the National Institutes Health through grants GM-56481 (J.P.Y.K.), P41-EB-2034 (G.M.R. and H.J.H), and CA-98757 (H.J.H.).

References

1. Elas M, Ahn KH, Parasca A, Barth ED, Lee D, Haney C, Halpern HJ. Electron paramagnetic resonance oxygen images correlate spatially and quantitatively with Oxylite oxygen measurements. Clin.Cancer Res 2006;12:4209–4217. [PubMed: 16857793]
2. Halpern, HJ.; Bowman, MK.; Eaton, GR.; Eaton, SS.; Ohno, K. EPR Imaging and in vivo EPR. CRC Press; Boca Raton, FL: 1991. Low Frequency EPR Spectrometers: MHz Range; p. 45-63.
3. Elas M, Bell R, Hleihel D, Barth ED, McFaul C, Haney CR, Bielanska J, Pustelny K, Ahn KH, Pelizzari CA, Kocherginsky M, Halpern HJ. Electron paramagnetic resonance oxygen image hypoxic fraction plus radiation dose strongly correlates with tumor cure in FSa fibrosarcomas. Int.J.Radiat.Oncol.Biol.Phys 2008;71:542–549. [PubMed: 18474313]
4. Halpern HJ, Chandramouli GV, Barth ED, Yu C, Peric M, Grdina DJ, Teicher BA. Diminished aqueous microviscosity of tumors in murine models measured with in vivo radiofrequency electron paramagnetic resonance. Cancer Res 1999;59:5836–5841. [PubMed: 10582707]
5. Khramstov VV, Weiner LM, Grigoriev IA, Volodarsky LB. Proton exchange in stable nitroxyl radicals. EPR study of the pH of aqueous solutions. Chem.Phys.Lett 1982:69–72.
6. Khramtsov VV, Yelinova VI, Weiner LM, Berezina TA, Martin VV, Volodarsky LB. Quantitative determination of SH groups in low- and high-molecular-weight compounds by an electron spin resonance method. Anal.Biochem 1989;182:58–63. [PubMed: 2557778]

7. Utsumi H, Yamada K, Ichikawa K, Sakai K, Kinoshita Y, Matsumoto S, Nagai M. Simultaneous molecular imaging of redox reactions monitored by Overhauser-enhanced MRI with 14N- and 15N-labeled nitroxyl radicals. Proc.Natl.Acad.Sci U.S.A 2006;103:1463–1468. [PubMed: 16432234]
8. Kao JP, Rosen GM. Esterase-assisted accumulation of 3-carboxy-2,2,5,5-tetramethyl-1-pyrrolidinyloxyl into lymphocytes. Org.Biomol.Chem 2004;2:99–102. [PubMed: 14737666]
9. Kao JP, Barth ED, Burks SR, Smithback P, Mailer C, Ahn KH, Halpern HJ, Rosen GM. Very-low-frequency electron paramagnetic resonance (EPR) imaging of nitroxide-loaded cells. Magn Reson.Med 2007;58:850–854. [PubMed: 17899588]
10. Rosen GM, Burks SR, Kohr MJ, Kao JP. Synthesis and biological testing of aminoxyls designed for long-term retention by living cells. Org.Biomol.Chem 2005;3:645–648. [PubMed: 15703801]
11. Shen J, Liu S, Miyake M, Liu W, Pritchard A, Kao JP, Rosen GM, Tong Y, Liu KJ. Use of 3-acetoxymethoxycarbonyl-2,2,5,5-tetramethyl-1-pyrrolidinyloxyl as an EPR oximetry probe: potential for in vivo measurement of tissue oxygenation in mouse brain. Magn Reson.Med 2006;55:1433–1440. [PubMed: 16680679]
12. Park JW, Hong K, Carter P, Asgari H, Guo LY, Keller GA, Wirth C, Shalaby R, Kotts C, Wood WI, et al. Development of anti-p185HER2 immunoliposomes for cancer therapy. Proc Natl Acad Sci U S A 1995;92:1327–1331. [PubMed: 7877976]
13. Park JW. Liposome-based drug delivery in breast cancer treatment. Breast Cancer Res 2002;4:95–99. [PubMed: 12052251]
14. Vaage J, Donovan D, Uster P, Working P. Tumour uptake of doxorubicin in polyethylene glycol-coated liposomes and therapeutic effect against a xenografted human pancreatic carcinoma. Br J Cancer 1997;75:482–486. [PubMed: 9052397]
15. Chan SW, Tan CT, Hsia JC. Spin membrane immunoassay: simplicity and specificity. J Immunol Methods 1978;21:185–195. [PubMed: 207779]
16. Begu S, Mordon S, Desmettre T, Devoisselle JM. Fluorescence imaging method for in vivo pH monitoring during liposomes uptake in rat liver using a pH-sensitive fluorescent dye. J Biomed Opt 2005;10:024008. [PubMed: 15910082]
17. Magin RL, Morse PD 2nd. Rapid measurement of drug release from temperature-sensitive liposomes by electron paramagnetic resonance and radioisotope techniques. Biochim Biophys Acta 1983;760:357–362. [PubMed: 6313067]
18. Chan HC, Magin RL, Swartz HM. Rapid assessment of liposomal stability in blood by an aqueous nitroxide spin label. J Biochem Biophys Methods 1989;18:271–276. [PubMed: 2550535]
19. Glockner JF, Norby SW, Swartz HM. Simultaneous measurement of intracellular and extracellular oxygen concentrations using a nitroxide-liposome system. Magn Reson Med 1993;29:12–18. [PubMed: 8380480]
20. Lee RJ, Wang S, Low PS. Measurement of endosome pH following folate receptor-mediated endocytosis. Biochim Biophys Acta 1996;1312:237–242. [PubMed: 8703993]
21. Daleke DL, Hong K, Papahadjopoulos D. Endocytosis of liposomes by macrophages: binding, acidification and leakage of liposomes monitored by a new fluorescence assay. Biochim Biophys Acta 1990;1024:352–366. [PubMed: 2162207]
22. Straubinger RM, Hong K, Friend DS, Papahadjopoulos D. Endocytosis of liposomes and intracellular fate of encapsulated molecules: encounter with a low pH compartment after internalization in coated vesicles. Cell 1983;32:1069–1079. [PubMed: 6404557]
23. Chin DJ, Straubinger RM, Acton S, Nathke I, Brodsky FM. 100-kDa polypeptides in peripheral clathrin-coated vesicles are required for receptor-mediated endocytosis. Proc Natl Acad Sci U S A 1989;86:9289–9293. [PubMed: 2574457]
24. Lee KD, Hong K, Papahadjopoulos D. Recognition of liposomes by cells: in vitro binding and endocytosis mediated by specific lipid headgroups and surface charge density. Biochim.Biophys.Acta 1992;1103:185–197. [PubMed: 1543703]
25. Bartlett GR. Phosphorus assay in column chromatography. J Biol Chem 1959;234:466–468. [PubMed: 13641241]
26. English LH, Epstein J, Cantley L, Housman D, Levenson R. Expression of an ouabain resistance gene in transfected cells. Ouabain treatment induces a K+-transport system. J.Biol.Chem 1985;260:1114–1119. [PubMed: 2981832]

27. Halpern HJ, Spencer DP, van Pole J, Bowman MK, Nelson AC, Dowey EM, Teicher BA. Imaging radio frequency electron-spin-resonance spectrometer with high resolution and sensitivity for in vivo measurements. Rev.Sci.Inst 1989;60:1040–1050.
28. Barrett, HH.; Wolf, E. Progress in Optics XXI. Elsevier Science; Amsterdam: 1984. The Radon transformation and its applications; p. 219-286.
29. Ahn KH, Halpern HJ. Simulation of 4D spectral-spatial EPR images. J.Magn Reson 2007;187:1–9. [PubMed: 17434772]
30. Fraley R, Straubinger RM, Rule G, Springer EL, Papahadjopoulos D. Liposome-mediated delivery of deoxyribonucleic acid to cells: enhanced efficiency of delivery related to lipid composition and incubation conditions. Biochemistry 1981;20:6978–6987. [PubMed: 6274382]
31. Straubinger RM, Hong K, Friend DS, Papahadjopoulos D. Endocytosis of liposomes and intracellular fate of encapsulated molecules: encounter with a low pH compartment after internalization in coated vesicles. Cell 1983;32:1069–1079. [PubMed: 6404557]
32. Keana JF, Pou S, Rosen GM. Nitroxides as potential contrast enhancing agents for MRI application: influence of structure on the rate of reduction by rat hepatocytes, whole liver homogenate, subcellular fractions, and ascorbate. Magn Reson Med 1987;5:525–536. [PubMed: 3437813]
33. Kocherginsky, N.; Swartz, HM. Nitroxide spin labels: reactions in biology and chemistry. CRC Press; Boca Raton, FL: 1995. Metabolism of nitroxides and thier products in cells; p. 126-135.
34. Tseng YL, Liu JJ, Hong RL. Translocation of liposomes into cancer cells by cell-penetrating peptides penetratin and tat: a kinetic and efficacy study. Mol.Pharmacol 2002;62:864–872. [PubMed: 12237333]
35. Pastorino F, Brignole C, Marimpietri D, Sapra P, Moase EH, Allen TM, Ponzoni M. Doxorubicin-loaded Fab' fragments of anti-disialoganglioside immunoliposomes selectively inhibit the growth and dissemination of human neuroblastoma in nude mice. Cancer Res 2003;63:86–92. [PubMed: 12517782]
36. Raffaghello L, Pagnan G, Pastorino F, Cosimo E, Brignole C, Marimpietri D, Bogenmann E, Ponzoni M, Montaldo PG. Immunoliposomal fenretinide: a novel antitumoral drug for human neuroblastoma. Cancer Lett 2003;197:151–155. [PubMed: 12880975]
37. Park JW, Hong K, Kirpotin DB, Meyer O, Papahadjopoulos D, Benz CC. Anti-HER2 immunoliposomes for targeted therapy of human tumors. Cancer Lett 1997;118:153–160. [PubMed: 9459205]
38. Eavarone DA, Yu X, Bellamkonda RV. Targeted drug delivery to C6 glioma by transferrin-coupled liposomes. J.Biomed.Mater.Res 2000;51:10–14. [PubMed: 10813739]
39. Iinuma H, Maruyama K, Okinaga K, Sasaki K, Sekine T, Ishida O, Ogiwara N, Johkura K, Yonemura Y. Intracellular targeting therapy of cisplatin-encapsulated transferrin-polyethylene glycol liposome on peritoneal dissemination of gastric cancer. Int.J.Cancer 2002;99:130–137. [PubMed: 11948504]
40. Lee RJ, Low PS. Folate-mediated tumor cell targeting of liposome-entrapped doxorubicin in vitro. Biochim.Biophys.Acta 1995;1233:134–144. [PubMed: 7865538]
41. Ni S, Stephenson SM, Lee RJ. Folate receptor targeted delivery of liposomal daunorubicin into tumor cells. Anticancer Res 2002;22:2131–2135. [PubMed: 12174894]
42. Liu F, Liu D. Serum independent liposome uptake by mouse liver. Biochim.Biophys.Acta 1996;1278:5–11. [PubMed: 8611606]
43. Woodle MC, Lasic DD. Sterically stabilized liposomes. Biochim.Biophys.Acta 1992;1113:171–199. [PubMed: 1510996]

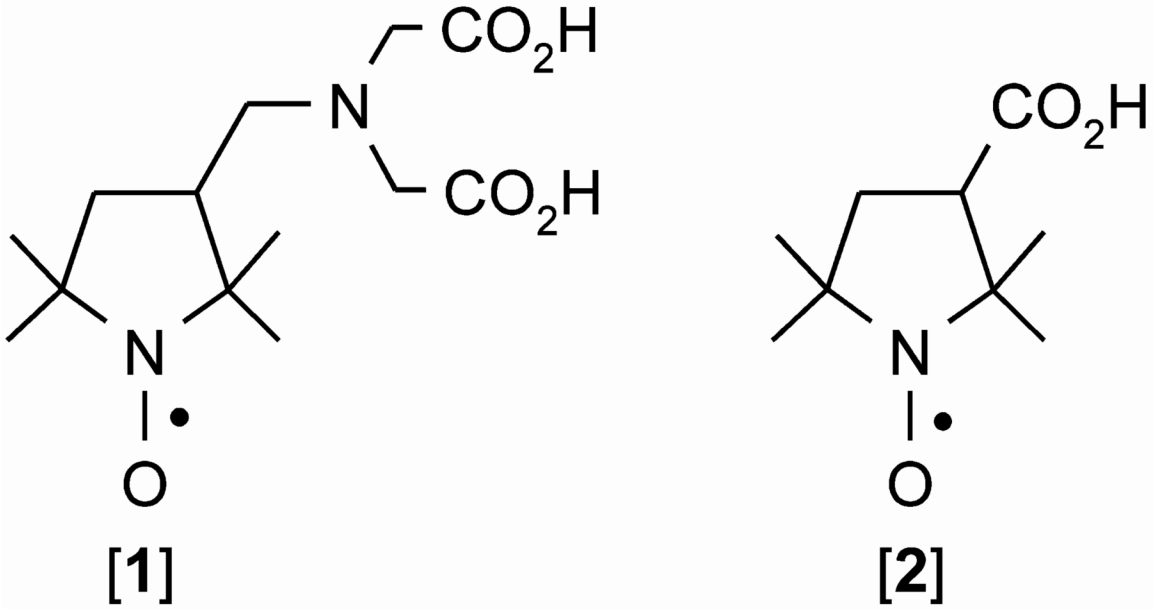

Figure 1.
Nitroxides used in the present study

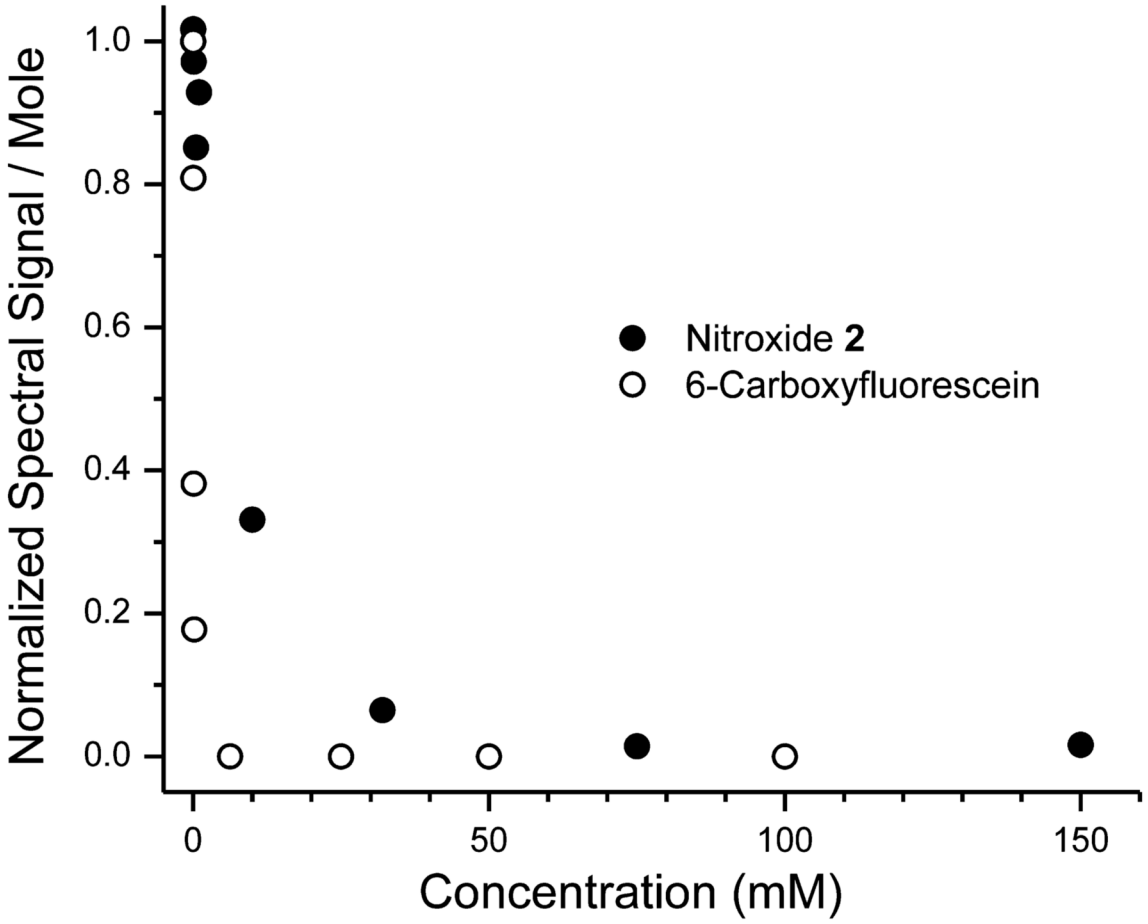

Figure 2.
Concentration–dependent quenching of 6-carboxyfluorescein, and nitroxide 2.

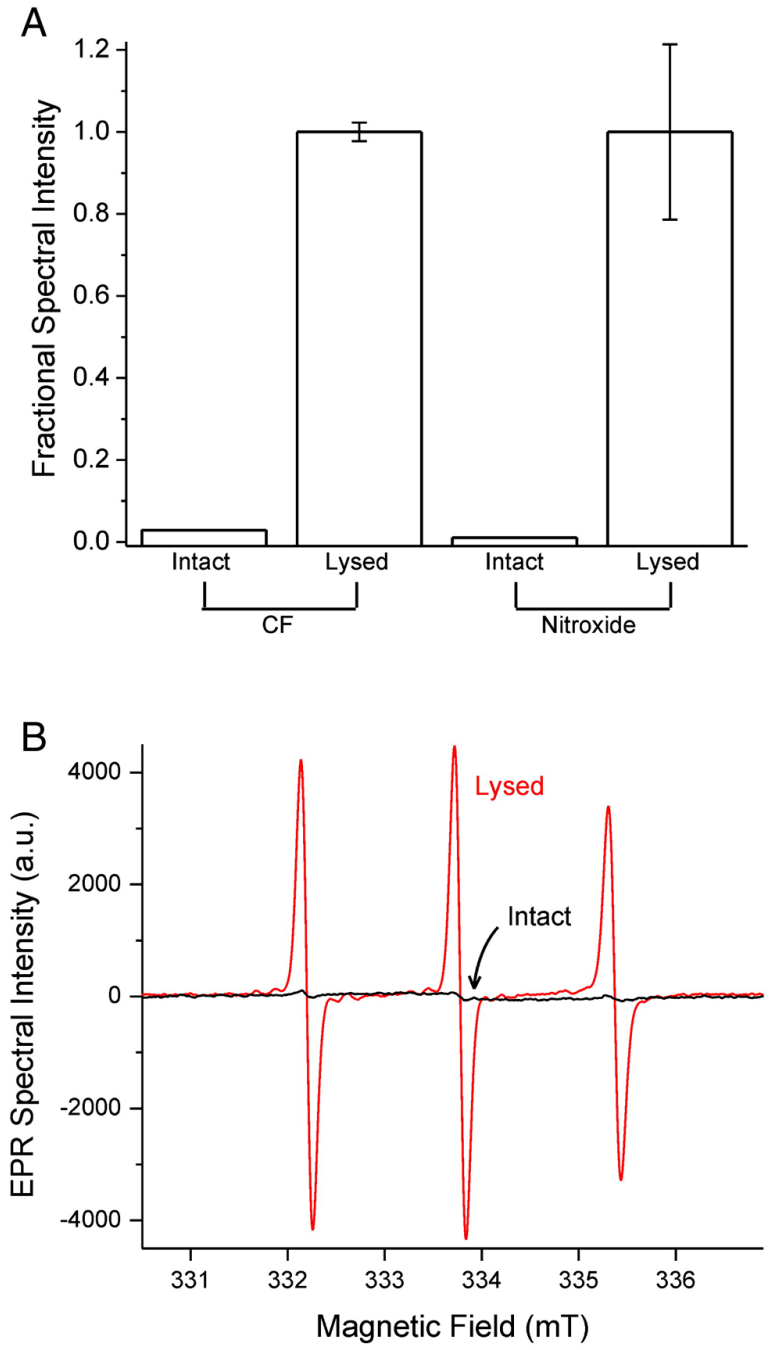

Figure 3. Intact liposomes encapsulating high probe concentrations are spectroscopically "dark"

(A) Spectroscopic signal intensity of suspensions of liposomes containing 100 mM CF or 150 mM nitroxide **1**, before and after lysis (n = 3; for visual clarity, error bars are omitted on the two "Intact" measurements, but both were < 12% of the mean value). (B) EPR spectra of liposomes encapsulating 150 mM nitroxide **1**. Intact liposomes (black trace) contain quenched nitroxide and show only a feeble EPR signal. Lysis releases nitroxides into bulk solution to produce a robust dequenched signal (red trace).

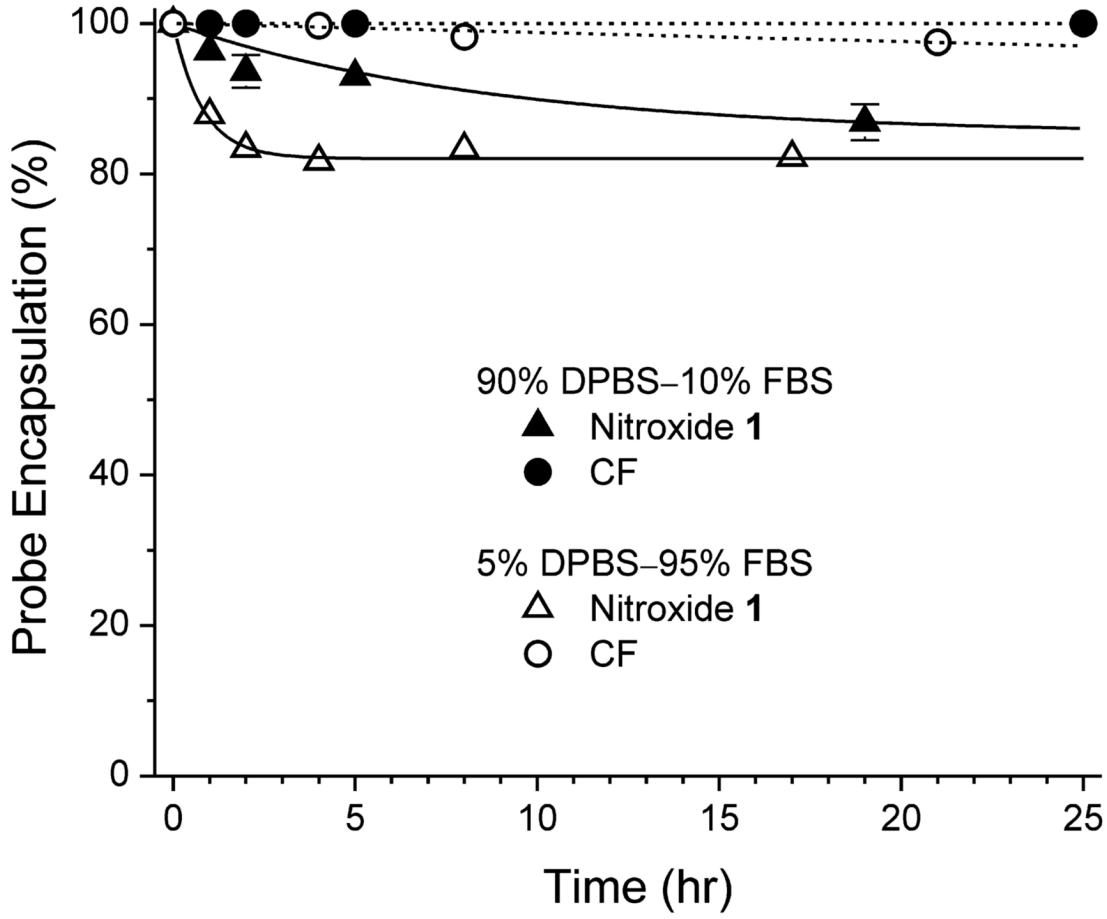

Figure 4. Liposomes containing quenched CF or nitroxide 1 are stable

At various times after preparation of liposomes, the amount of CF or nitroxide **1** remaining encapsulated was assayed. In 90% DPBS–10% FBS, the data for CF-containing liposomes (filled circles) are well fit by a line with a slope of -2.0×10^{-4} %/hr (dashed line), whereas the data for nitroxide-containing liposomes (filled triangles) are well fit by a first-order exponential decay to a baseline of 85.2% with a time constant of $\tau = 8.7$ hr (solid curve). In 5% DPBS–95% FBS, the data for CF-containing liposomes (open circles) are well fit by a line with a slope of -0.12 ± 0.011 % / hr (dashed line), whereas the data for nitroxide-containing liposomes (open triangles) are well fit by a first-order exponential decay to a baseline of 82.1% with a time constant of $\tau = 0.81 \pm 0.068$ hr (solid curve). Each data point is the mean of three samples. Where not shown, the error bar is smaller than the symbol.

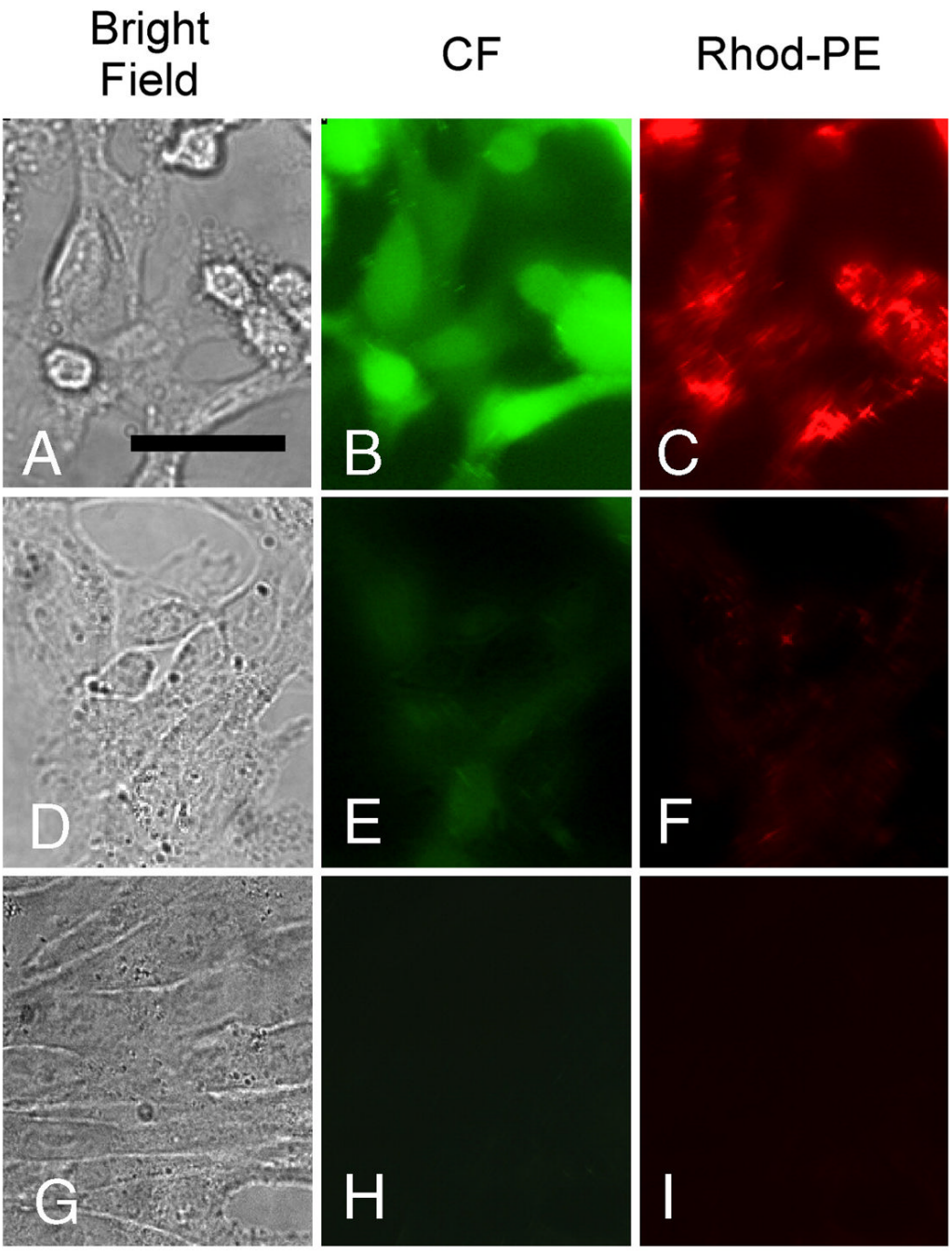

Figure 5. Fluorescence images of CV1 cells incubated with Rhod-PE–containing liposomes encapsulating CF

Panels A, D and G are brightfield images; panels B, E and H are images acquired in the CF fluorescence channel; panels C, F and I are images acquired in the Rhod-PE channel. Scale bar in panel A represents 20 μm. Cells avidly endocytosed PS-bearing (negatively charged) liposomes at 37 °C, leading to bright intracellular CF and Rhod-PE signals (A-C). In contrast, neutral liposomes (bearing no PS) are poorly endocytosed at 37 °C (D–F). Endocytosis of negatively charged liposomes is blocked at 4° C, resulting in no observable uptake of CF or Rhod-PE (G–I).

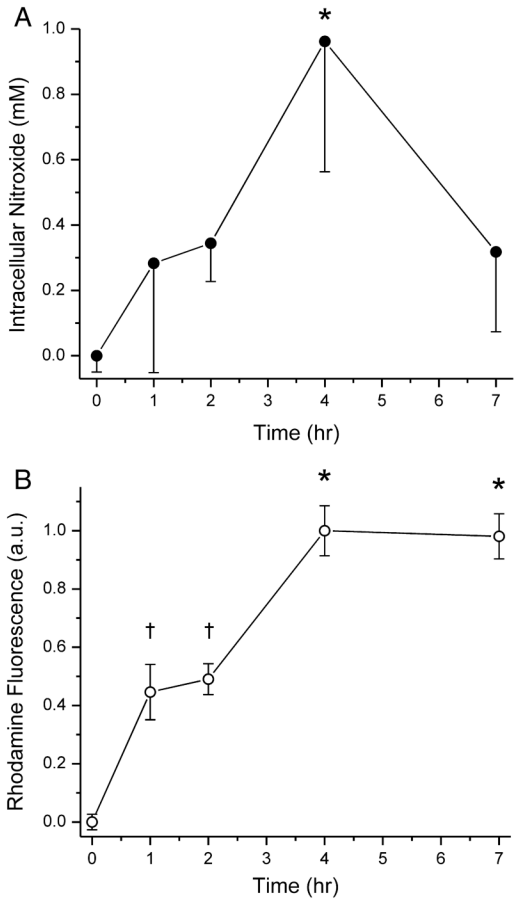

Figure 6. Cellular uptake of Rhod-PE–containing liposomes encapsulating nitroxide 1

Dishes of CV1 cells were incubated at 37° C with liposomes containing PS and Rhod-PE and loaded with nitroxide **1**. At various times, intracellular nitroxide (A) and Rhod-PE (B) were assayed spectroscopically. After 4 hr, intracellular nitroxide concentration increased to ~1 mM through liposomal endocytosis, as verified by a parallel uptake of liposomal Rhod-PE. Beyond 4 hr, endocytosis slowed (as evidenced by the lack of further Rhod-PE accumulation), and there was a decline of intracellular nitroxide signal. In panel A, only down error bars are shown. Statistical significance ($p < 0.05$) is denoted by asterisks and daggers. ANOVA values: panel A, $F_{4,18} = 6.99$; panel B, $F_{4,14} = 66.15$. Each point is the average from assaying 3 – 4 dishes of cells.

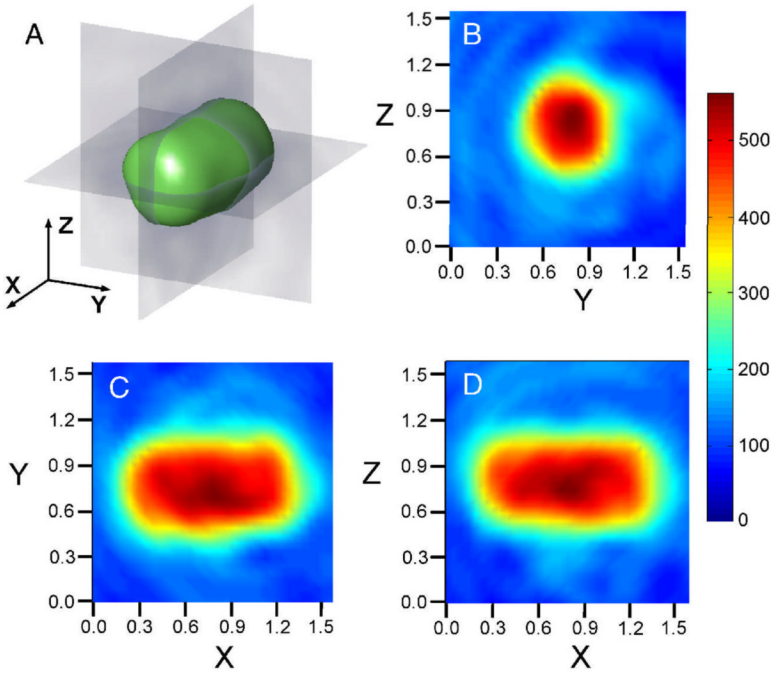

Figure 7. EPR image of an agarose cylinder impregnated with 400 μM nitroxide 1 and implanted in a mouse

(A) Surface intensity plot of the cylinder with cross-sectional planes shown in gray. (B-D) Cross-sectional views of the cylinder at the planes indicated in panel A. All axis labels are in units of cm. Intensity is encoded according to the pseudocolor scale shown at right.